
GIST: Distributed Training for Large-Scale Graph Convolutional Networks

Cameron R. Wolfe^{*1} Jinkang Yang^{*2} Arindam Chowdhury³ Chen Dun¹ Artun Bayer³ Santiago Segarra³
Anastasios Kyriillidis¹

Abstract

The graph convolutional network (GCN) is a go-to solution for machine learning on graphs, but its training is notoriously difficult to scale in terms of both the size of the graph and the number of model parameters. These limitations are in stark contrast to the increasing scale (in data size and model size) of experiments in deep learning research. In this work, we propose GIST, a novel distributed approach that enables efficient training of wide (overparameterized) GCNs on large graphs. GIST is a hybrid layer and graph sampling method, which disjointly partitions the global model into several, smaller sub-GCNs that are independently trained across multiple GPUs in parallel. This distributed framework improves model performance and significantly decreases wall-clock training time. GIST seeks to enable large-scale GCN experimentation with the goal of bridging the existing gap in scale between graph machine learning and deep learning.

1. Introduction

Background. Since not all data can be adequately represented in Euclidean space (Bronstein et al., 2017), a large number of applications rely on graph-structured data. For example, social networks can be modeled by regarding each user as a node in a graph where edges represent friendship relations (Newman et al., 2002; Lusher et al., 2013). Alternatively, in chemistry, molecules can be modeled as graphs, with nodes representing atoms and edges encoding chemical bonds (Balaban, 1985; Benkő et al., 2003).

To better understand graph-structured data, several (deep) learning techniques have been extended to the graph do-

main (Gori et al., 2005; Masci et al., 2015; Defferrard et al., 2016). Currently, the most popular one is the graph convolutional network (GCN) (Kipf & Welling, 2016), a multi-layer architecture that implements a generalization of the convolution operation to graphs.

Although the GCN is effective at node and graph-level classification, it is notoriously inefficient and unable to handle large-scale graphs (Zeng et al., 2019; Gao et al., 2018; Huang et al., 2018; Chen et al., 2018b;a; You et al., 2020). The convolution operation on a graph incorporates information within neighborhoods, whose size increases with the depth of the model. This results in high computational costs that grow exponentially with the number of layers. Furthermore, these methods incur a high memory cost in loading the entire graph and node embeddings for the duration of training. Thus, GCN training is very susceptible to memory overflow and the scale of experiments is quite limited (i.e., both models and graphs are restricted in size).

To deal with these issues, efficient GCN training has been heavily investigated, sparking the development of node partitioning methodologies. These schemes can be roughly categorized into neighborhood sampling (Hamilton et al., 2017; Chen et al., 2018a; Zou et al., 2019) and graph partitioning (Chiang et al., 2019; Zeng et al., 2019) approaches. The goal is to partition a large graph into multiple smaller graphs that can be used to train the GCN, thus allowing for the formation of mini-batches. In this way, GCNs gain the ability to handle larger graphs during training, thus expanding their potential into the realm of big data.

Motivation. Although some papers illustrate large-scale GCN experiments (Chiang et al., 2019; Zeng et al., 2019), the models (and data) used in GCN research remain small in comparison to main-stream deep learning research (Veličković et al., 2017; Kipf & Welling, 2016). Formative publications in the area even hinted at the challenge of training larger (deeper) models (Kipf & Welling, 2016). In contrast, recent deep learning research has revealed that severely overparameterized models can discover generalizable solutions (Nakkiran et al., 2019), creating a trend toward larger models and datasets (Brown et al., 2020; Conneau et al., 2019). These findings motivate the exploration of larger models and datasets for machine learning on graphs.

^{*}Equal contribution ¹Department of Computer Science, Rice University, Houston, TX, USA. ²School of Computer Science and Engineering, Nanyang Technology University, Singapore. ³Department of Electrical and Computer Engineering, Rice University, Houston, TX, USA.. Correspondence to: Cameron Wolfe <crw13@rice.edu>.

This paper. We propose a hybrid *layer* and *graph* sampling approach for distributed, multi-GPU training of GCNs. More precisely, we partition the hidden feature space in each *layer* to effectively decompose a global GCN model into multiple, narrow sub-GCNs of equal depth. Moreover, especially for large graphs, we partition the *graph* into densely connected subgraphs and train the sub-GCNs on these subgraphs. Sub-GCNs are trained independently for several iterations, prior to having their updates synchronized. Then, a new group of sub-GCNs is created (through a different random realization of layer sampling), trained, and synchronized. This process is repeated until convergence. We call this method graph independent subnetwork training (GIST). GIST significantly reduces the wall-clock time of large-scale GCN experiments, allowing larger models and datasets to be explored.

Our main contributions can be summarized as follows:

- i)* We develop the first independent sub-GCN training scheme by combining the partitions of the hidden feature space and the graph being analyzed.
- ii)* We illustrate how GIST can be used to either achieve state-of-the-art performance with faster training or surpass existing benchmarks by enabling the training of markedly overparameterized GCN models. In particular, GIST is successfully used to train a two-layer GCN model with a hidden dimension of 32,768 on the Amazon2M dataset.
- iii)* We provide PyTorch (Paszke et al., 2019) implementations of GIST both for the vanilla GCN (Kipf & Welling, 2016) and GraphSAGE (Hamilton et al., 2017).

2. What is the GIST of this work?

The GCN (Kipf & Welling, 2016) is arguably the most widely-used neural network architecture on graphs. Consider a graph \mathcal{G} comprised of n nodes with d -dimensional features $\mathbf{X} \in \mathbb{R}^{n \times d}$. The output $\mathbf{Y} \in \mathbb{R}^{n \times d'}$ of a GCN can be expressed as $\mathbf{Y} = \Psi_{\mathcal{G}}(\mathbf{X}; \Theta)$, where $\Psi_{\mathcal{G}}$ is a layered architecture with trainable parameters Θ . If we define $\mathbf{H}_0 = \mathbf{X}$, we then have that $\mathbf{Y} = \Psi_{\mathcal{G}}(\mathbf{X}; \Theta) = \mathbf{H}_L$, where an intermediate ℓ -th layer of the GCN is given by

$$\mathbf{H}_{\ell+1} = \sigma(\bar{\mathbf{A}} \mathbf{H}_{\ell} \Theta_{\ell}). \quad (1)$$

In (1), σ is an elementwise activation function (e.g., ReLU), $\bar{\mathbf{A}}$ is the degree-normalized adjacency matrix of \mathcal{G} with added self-loops, and the trainable parameters $\Theta = \{\Theta_{\ell}\}_{\ell=0}^{L-1}$ have dimensions $\Theta_{\ell} \in \mathbb{R}^{d_{\ell} \times d_{\ell+1}}$ with $d_0 = d$ and $d_L = d'$. For illustrative purposes, we focus on the case of $L = 3$ layers; in Figure 2-(top), we show the explicit version of the nested layers in (1). However, our methodology extends seamlessly to arbitrary L ; see Section 4. The activation function σ is typically chosen as the identity or softmax function in the last layer. For simplicity, we omit this in Figure 2.

GIST overview. We present a high-level overview of GIST in Algorithm 1. A schematic depiction of Algorithm 1 is also provided in Figure 1.

Algorithm 1 GIST Algorithm

Parameters: T synchronization iterations, m sub-GCNs, ζ local iterations, c clusters, \mathcal{G} training graph.

$\Psi_{\mathcal{G}}(\cdot; \Theta) \leftarrow$ randomly initialize GCN

$\{\mathcal{G}_{(j)}\}_{j=1}^c \leftarrow \text{Cluster}(\mathcal{G}, c)$

for $t = 0, \dots, T - 1$ **do**

$\{\Psi_{\mathcal{G}}(\cdot; \Theta^{(i)})\}_{i=1}^m \leftarrow \text{subGCNs}(\Psi_{\mathcal{G}}(\cdot; \Theta), m)$

Distribute each $\Psi_{\mathcal{G}}(\cdot; \Theta^{(i)})$ to a different worker

for $i = 1, \dots, m$ **do**

for $z = 1, \dots, \zeta$ **do**

$\Psi_{\mathcal{G}}(\cdot; \Theta^{(i)}) \leftarrow \text{subTrain}(\Theta^{(i)}, \{\mathcal{G}_{(j)}\}_{j=1}^c)$

end for

end for

$\Psi_{\mathcal{G}}(\cdot; \Theta) \leftarrow \text{subAgg}(\{\Theta^{(i)}\}_{i=1}^m)$

end for

After a random initialization of the (global) GCN model, our graph domain is partitioned into c clusters through the `Cluster` function ($c = 2$ in Figure 1). This operation is particularly relevant for large graphs ($n > 50,000$), and we omit it ($c = 1$) for smaller graphs that can be efficiently handled without partitioning. Though any clustering method can be used, we advocate the use of METIS (Karypis & Kumar, 1998b;a) due to its proven efficiency in large-scale graphs. We then partition our global GCN into m smaller and disjoint sub-GCNs through the `subGCNs` function ($m = 2$ in Figure 1 and Figure 2). This partition is achieved by sampling the feature space at the different layers of the GCN; see Section 2.1 for details. Each sub-GCN is assigned to a different worker (i.e., a different GPU) for ζ rounds of distributed and independent training through `subTrain`. After this, newly-learned sub-GCN parameters are aggregated (`subAgg`) into the global GCN model. Then, the global model is again split into sub-GCNs and the process repeats for T cycles or until a pre-specified stopping criterion is met. More details on distributed training and aggregation are given in Section 2.2.

2.1. subGCNs: Constructing Sub-GCNs

GIST operates by partitioning a global GCN model into several narrower sub-GCNs of equal depth. This is attained by partitioning the (hidden) feature spaces at different layers. Formally, consider an arbitrary layer ℓ and a random partition of the feature set $[d_{\ell}] = \{1, 2, \dots, d_{\ell}\}$ into m equally-sized blocks $\{\mathcal{D}_{\ell}^{(i)}\}_{i=1}^m$. E.g., if $d_{\ell} = 4$ and $m = 2$, one valid partition would be given by $\mathcal{D}_{\ell}^{(1)} = \{1, 4\}$ and $\mathcal{D}_{\ell}^{(2)} =$

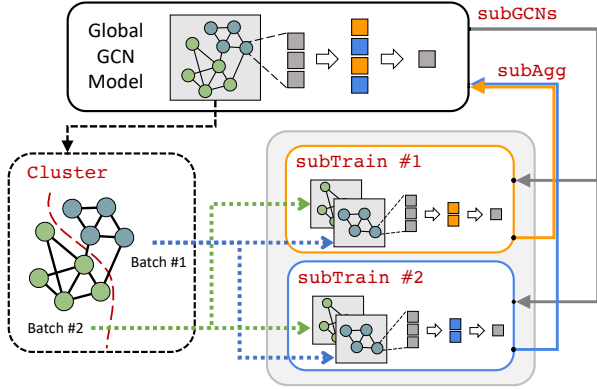


Figure 1. Pipeline for the proposed GIST. `subGCNs` divides the global GCN into several sub-GCNs. Every sub-GCN is trained by `subTrain` using mini-batches. These mini-batches are generated by `Cluster`, which pre-processes the training graph into several smaller sub-graphs. Parameters of the sub-GCNs are intermittently aggregated with the global model through `subAgg`.

$\{2, 3\}$. Accordingly, we denote by $\Theta_\ell^{(i)} = [\Theta_\ell]_{\mathcal{D}_\ell^{(i)} \times \mathcal{D}_{\ell+1}^{(i)}}$ the matrix obtained by selecting from Θ_ℓ the rows and columns given by the i th blocks in the partitions of $[d_\ell]$ and $[d_{\ell+1}]$, respectively. With this notation in place, we can define m different sub-GCNs $\mathbf{Y}^{(i)} = \Psi_{\mathcal{G}}(\mathbf{X}^{(i)}; \Theta^{(i)}) = \mathbf{H}_L^{(i)}$ where $\mathbf{H}_0^{(i)} = \mathbf{X}_{[m] \times \mathcal{D}_0^{(i)}}$ and each layer is given by:

$$\mathbf{H}_{\ell+1}^{(i)} = \sigma(\bar{\mathbf{A}} \mathbf{H}_\ell^{(i)} \Theta_\ell^{(i)}). \quad (2)$$

This partition into sub-GCNs is illustrated in Figure 2-(a) where $m = 2$ and the two different blocks in each partition are depicted by the orange and blue colors. Notice that the input data \mathbf{X} is only partitioned columnwise, whereas a generic weight matrix Θ_ℓ is partitioned across both dimensions, leading to a substantially reduced complexity of the sub-GCNs in (2) compared with the original GCN in (1). More precisely, the weight matrix $\Theta_\ell^{(i)}$ is of size $d_\ell/m \times d_{\ell+1}/m$, leading to a reduction of order m^2 in the number of parameters where, for simplicity, we assume that d_ℓ is divisible by m for all ℓ . *This marked decrease in the model complexity of the sub-GCNs compared with the original GCN is a major source of accelerated training.*

We give particular consideration to the partition of the input $d_0 = d$ and output $d_L = d'$ feature dimensions. We do not partition the output feature space so that the output dimensions of a generic sub-GCN $\mathbf{Y}^{(i)}$ coincide with the output dimensions of the original GCN, \mathbf{Y} . In this way, there is no need to modify the loss function when performing sub-GCN training. For this reason, the columns of Θ_3 are not partitioned in Figure 2-(a). We also advocate for the input dimension not to be partitioned; see Figure 2-(b) and Table 2 for in-depth explanation. Notice that, as previously stated, the above procedure can be trivially extended to arbi-

trarily deep GCNs. This decomposition scheme is denoted by `subGCNs` in Algorithm 1.

2.2. `subTrain` and `subAgg`: Sub-GCN Training

Once sub-GCNs are constructed as described in Section 2.1, training is conducted independently for several iterations in a synchronous manner (`subTrain`) and the results are then aggregated back into the global GCN model (`subAgg`).

First, assume $c = 1$ so that the `Cluster` operation in Algorithm 1 is moot and $\{\mathcal{G}_{(j)}\}_{j=1}^c = \mathcal{G}$. Recall from Section 2.1 that the output $\mathbf{Y}^{(i)}$ of every sub-GCN has the same dimensions as the output of the global model, thus, each sub-GCN can be trained to minimize the same global loss function considered for the learning problem of interest. In this way, GIST is flexible by being agnostic to the specific loss function chosen by the practitioner. Then, one application of `subTrain` in Algorithm 1 corresponds to one step of stochastic gradient descent. This synchronous and independent training of sub-GCNs is inspired by local SGD (Lin et al., 2018) and is conducted on separate GPUs, facilitating a parallelized implementation.

The number of independent training iterations between synchronization rounds, referred to as local iterations, is given by the hyperparameter ζ . In general, for a fixed total number of stochastic gradient descent steps, more local iterations reduce the communication costs between GPUs. Furthermore, the total amount of training is split across sub-GCNs. For example, if a global model is trained on a single GPU for 10 epochs, a comparable experiment for GIST with two sub-GCNs would train each sub-GCN for only 5 epochs. Ideally, one would want to increase the number of sub-GCNs and local iterations as much as possible, as this decreases the wall-clock time required to complete a fixed number of epochs. In practice, however, such training acceleration will be diminished by communication requirements and may come at the cost of degraded model performance (see Section 4.1); further, the number of sub-GCNs is upper-bounded by the number of GPUs for parallel training.

Consider now the case when $c > 1$. In this setting, `subTrain` first selects one of the c subgraphs in $\{\mathcal{G}_{(j)}\}_{j=1}^c$, which will be used as a mini-batch for the computation of the stochastic gradient descent step. This allows our methodology to easily generalize to large-scale graphs. Alternatively, several sub-graphs can be chosen from $\{\mathcal{G}_{(j)}\}_{j=1}^c$ and use their union as a mini-batch for training. It should be noted that such pre-processing of a large training graph into computationally-tractable sub-graphs for use during training resembles the methodology followed by `ClusterGCN` (Chiang et al., 2019). This pipeline is illustrated in Figure 1 for $c = 2$ clusters and $m = 2$ sub-GCNs. In each application of `subTrain`, a sub-GCN is trained on either the green or the blue subgraph and a single stochastic

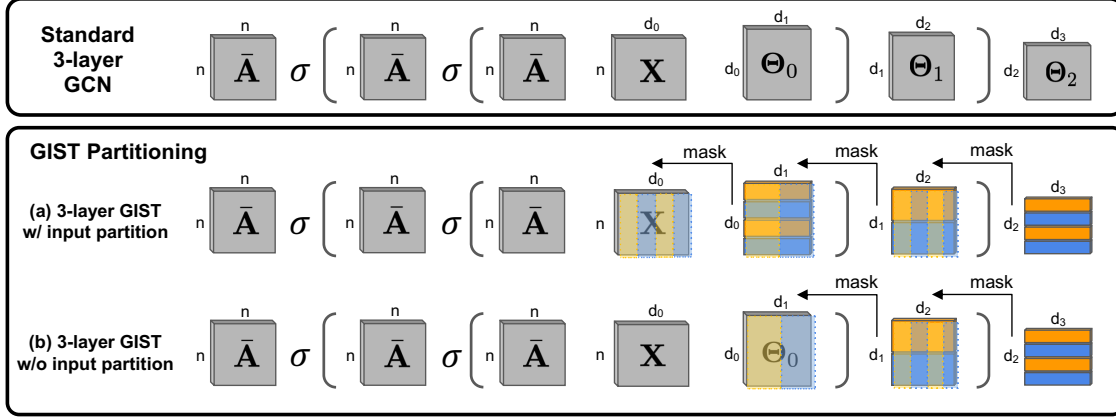


Figure 2. Diagram of the proposed partition of a (global) GCN model into $m = 2$ sub-GCNs (subGCNs in Algorithm 1). The partition of the feature dimensions is given by the orange and blue colors. While both hidden dimensions (d_1 and d_2) are partitioned, the output dimension d_3 is not partitioned, and we consider (a) partitioning and (b) not partitioning the input dimension d_0 .

gradient descent step is taken.

When each sub-GCN has finished training for ζ iterations, their updates are aggregated into the global model through the `subAgg` function in Algorithm 1. Recall that the feature space at different layers is partitioned disjointly between workers, i.e., $\mathcal{D}_\ell^{(i)} \cap \mathcal{D}_\ell^{(j)} = \emptyset$ for $i \neq j$ and for all ℓ . Hence, each worker simply replaces the corresponding entries in the global parameters Θ with its own parameters $\Theta^{(i)}$, where the aforementioned disjoint partition guarantees that no collisions will occur.

Notice that not every parameter Θ in the global GCN model will be updated with each application of `subAgg`, since not every parameter is assigned to some worker through subGCNs. This can be readily seen if we focus on Θ_1 in Figure 2-(a), where one worker will be assigned $\Theta_1^{(1)}$ formed by the two orange rectangular blocks and the other worker will be assigned $\Theta_1^{(2)}$ formed by the two blue rectangular blocks, whereas the rest of Θ_1 will not be assigned to any worker. Hence, these non-assigned parameters would not be updated by `subAgg`. Nonetheless, since the partition into sub-GCNs is randomly drawn in each cycle t , one expects all of Θ to be updated multiple times for large T .

From the above description it follows that the global GCN model is never trained directly in GIST, but is rather updated through the training of sub-GCNs. Moreover, the feature dimensions of each sub-GCN are a factor of m smaller than the global model at each layer, leading to an overall reduction of m^2 in the number of parameters. Consequently, GIST can be used to train global GCN models that typically exceed the capacity of a single GPU as long as each sub-GCN can be trained in a GPU. In particular, the global model can have hidden feature dimensions that are a factor of m larger than the largest model that can be trained in a single GPU. In this way, GIST cannot only be used

to accelerate the training of existing models but can also be used to train markedly overparametrized (“ultra-wide”) GCN models. In Section 4.2 we show that by relying on this capability of GIST, we can train a two-layer GCN model with a hidden dimension of 32,768 to high performance on the Amazon2M dataset.

2.3. Implementation Details

We provide an implementation of GIST in PyTorch (Paszke et al., 2019) using the NCCL distributed communication package. Moreover, apart from the implementation for the vanilla GCN as introduced in (1), we also provide an implementation of GIST for GraphSAGE (Hamilton et al., 2017), another widely-used graph neural network. The implementation for both graph neural networks is centralized, meaning that a single process serves as a central parameter server. From this central process, the weights of the global model are maintained and partitioned to different worker processes (including itself) for independent training. All experiments are conducted on a machine with 8 NVIDIA Tesla V100-PCIE-32G GPU, 56-core Intel(R) Xeon(R) CPU E5-2680 v4 @ 2.40GHz, and 256 GB of RAM.

3. Related Work

GCN training. In spite of their widespread success in several graph related tasks, GCNs often suffer from training inefficiencies (Gao et al., 2018; Huang et al., 2018). Consequently, the research community has focused on developing efficient and scalable algorithms for training GCNs (Chen et al., 2018b; Hamilton et al., 2017; Chen et al., 2018a; Zou et al., 2019; Chiang et al., 2019; Zeng et al., 2019). The resulting approaches can be divided roughly into two areas: *neighborhood sampling* and *graph partitioning*. However, it is important to note that these two broad classes of solutions

are not mutually exclusive, and reasonable combinations of the two approaches may be beneficial.

Neighborhood sampling methodologies aim to sub-select neighboring nodes at each layer of the GCN, thus limiting the number of node representations in the forward pass and mitigating the exponential expansion of the GCNs receptive field. VRGCN (Chen et al., 2018b) implements a variance reduction technique to reduce the sample size in each layer, which achieves good performance with smaller graphs. However, it requires to store all the intermediate node embeddings during training, leading to a memory complexity close to full-batch training. GraphSAGE (Hamilton et al., 2017) learns a set of aggregator functions to gather information from a node’s local neighborhood. It then concatenates the outputs of these aggregation functions with each node’s own representation at each step of the forward pass. FastGCN (Chen et al., 2018a) adopts a Monte Carlo approach to evaluate the GCN’s forward pass in practice, which computes each node’s hidden representation using a fixed-size, randomly-sampled set of nodes. LADIES (Zou et al., 2019) introduces a layer-conditional approach for node sampling, which encourages node connectivity between layers in contrast to FastGCN (Chen et al., 2018a).

Graph partitioning schemes aim to select densely-connected sub-graphs within the training graph, which can be used to form mini-batches during GCN training. Such sub-graph sampling reduces the memory footprint of GCN training, thus allowing larger models to be trained over graphs with many nodes. ClusterGCN (Chiang et al., 2019) produces a very large number of clusters from the global graph, then randomly samples a subset of these clusters and computes their union to form each sub-graph or mini-batch. Similarly, GraphSAINT (Zeng et al., 2019) randomly samples a sub-graph during each GCN forward pass. However, GraphSAINT also considers the bias created by unequal node sampling probabilities during sub-graph construction, and proposes normalization techniques to eliminate this bias.

As explained in Section 2, GIST also relies on graph partitioning techniques (Cluster) to handle large graphs. However, the feature sampling scheme at each layer (subGCNs) that leads to parallel and narrower sub-GCNs is a hitherto unexplored framework for efficient GCN training.

Distributed training. Distributed training is a heavily studied topic (Shi et al., 2020; Zhang et al., 2018). Our work focuses on synchronous and distributed training techniques (Zhang et al., 2015; Lian et al., 2017; Yu et al., 2019). Some examples of synchronous, distributed training approaches include data parallel training, parallel SGD (Zinkevich et al., 2010; Agarwal & Duchi, 2011), and local SGD (Lin et al., 2018; Stich, 2019). Our methodology holds similarities to model parallel training techniques, which have been heavily explored (Ben-Nun & Hoefler, 2019;

Gholami et al., 2017; Zhu et al., 2020; Kirby et al., 2020; Tavarageri et al., 2019; Pauloski et al., 2020; Günther et al., 2018). More closely, our approach is inspired by independent subnetwork training (Yuan et al., 2019), explored for multi-layer perceptrons.

4. Experiments

We extensively explore GIST by performing multi-class node classification on five publicly available datasets; see Table 1. We adopt standard training, validation, and testing splits. In all experiments, we compare the performance of GIST to that of single-GPU baseline models, but comparisons of GIST to other distributed training methodologies (e.g., local SGD (Lin et al., 2018) and ensembles) are also provided in the supplementary material. Cora, Citeseer, and Pubmed are considered “small-scale” datasets and are used to run low-cost ablation experiments; see Section 4.1. Reddit and Amazon2M are considered “large-scale” datasets. F1 score and training time are used to measure the performance of GIST for both of these datasets; see Section 4.2. For large-scale datasets, the goal of GIST is to *i*) achieve state-of-the-art performance, *ii*) minimize wall-clock training time, and *iii*) enable experiments with very large GCN models.

Table 1. Statistical details of datasets for GIST experiments.

Dataset	n	# Edges	# Labels	d
Cora (Sen et al., 2008)	2,708	5,429	7	1,433
CiteSeer (Sen et al., 2008)	3,312	4,723	6	3,703
Pubmed (Sen et al., 2008)	19,717	44,338	3	500
Reddit (Hamilton et al., 2017)	232,965	11.6 M	41	602
Amazon2M (Chiang et al., 2019)	2.5 M	61.8 M	47	100

4.1. Small-Scale Experiments

In this section, we present several numerical experiments conducted over the Cora, Citeseer, and Pubmed datasets (Sen et al., 2008) with GIST. Because the datasets in these experiments are small, no wall-clock speedup is observed. As a result, we exclude speed measurements from this analysis. All experiments are run for a total of 400 epochs with a step learning rate schedule that decays the learning rate by $10\times$ at 50% and 75% of total epochs. A vanilla GCN model, as described in (Kipf & Welling, 2016), is used. The model is trained in a full-batch manner using the Adam optimizer (Kingma & Ba, 2014), and all reported results are averaged across five trials with different random seeds. For all L -layer models considered, we have that d_0 and d_L are respectively given by the number of features and output classes in the dataset being studied (see Table 1), whereas the size of every hidden layer d_1 through d_{L-1} is the same, and varies across experiments.

Single-GPU Models. We begin by testing different baseline models over the small-scale datasets. Models with different depths (L) and hidden dimensions are tested using a single

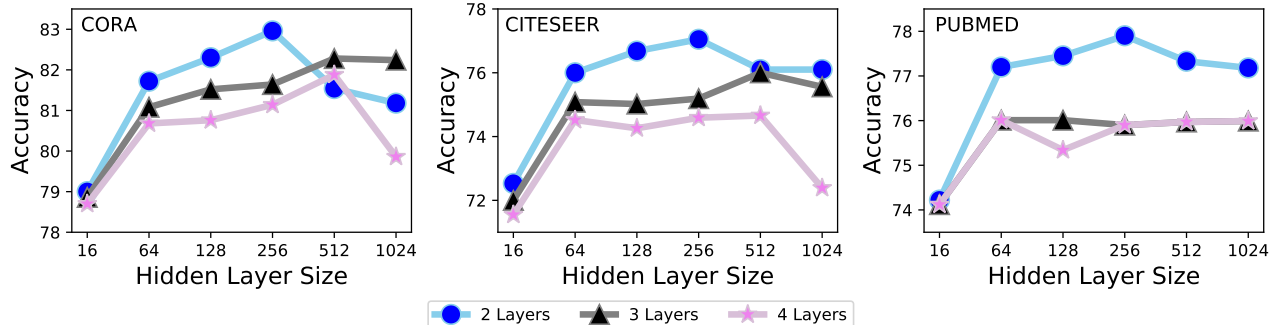


Figure 3. Test accuracy for different sizes (i.e., varying depth and width) of single-GPU GCN models across small-scale datasets.

GPU. The results are shown in Figure 3. As can be seen, deeper models do not yield performance improvements for small-scale datasets. However, test accuracy tends to improve as the model becomes wider. Based upon the results in Figure 3 and unless otherwise stated, we adopt as our *baseline* a 3-layer GCN model with a hidden dimension of $d_1 = d_2 = 256$ for all the small-scale experiments. Though 2-layer models seem to perform best, we use a 3-layer model as our baseline to enable more flexibility in examining the partitioning strategy of GIST.

Which layers should be partitioned? We investigate whether GIST is sensitive to the partitioning of certain layers when generating the sub-GCNs. Ideally, partitioning all (hidden) feature dimensions would yield the greatest acceleration (i.e., less communication and smaller model), but this speedup may come at the cost of degraded model performance. While partitioning the first hidden dimension d_1 , we study the impact on performance of partitioning the input dimension d_0 and the second hidden dimension d_2 . Recall that we do not partition the output dimension d_3 so that each sub-GCN still outputs a prediction in the label space. The results of such partitioning tests are displayed in Table 2.

Table 2. Test accuracy of a 3-layer GCN of width 256 trained with GIST. Input and hidden layers are selectively partitioned so that the performance impact of partitioning each separate layer can be observed. A check mark indicates that a certain feature dimension is partitioned, whereas no check mark indicates that the whole dimension is shared between sub-GCNs.

# Sub-GCNs	d_0	d_1	d_2	Cora	Citeseer	Pubmed
Baseline				81.52	75.02	75.90
2	✓	✓	✓	80.16	75.95	76.40
	✓	✓	✓	80.90	75.88	76.43
		✓	✓	80.82	75.82	76.26
4	✓	✓	✓	74.70	73.36	72.15
	✓	✓	✓	77.16	74.68	74.05
		✓	✓	81.18	76.21	76.73
8	✓	✓	✓	46.40	44.55	47.57
	✓	✓	✓	53.60	54.68	54.47
		✓	✓	79.58	75.39	75.98

Partitioning the input weight matrix leads to a significant decrease in test accuracy for all datasets as we consider

a larger number m of sub-GCNs. E.g., when $m = 8$, an accuracy of 79.58% is attained for the Cora dataset when both hidden dimensions are partitioned but the input is not, whereas this accuracy drastically drops to 46.40% if the input dimensions d_0 is also partitioned. Intuitively, this performance decrease occurs because, in the latter case, each sub-GCN observes only a portion of node input features (i.e., each sub-GCN has a d_0/m -dimensional input). Table 2 also reveals that hidden dimensions can be partitioned all the way to $m = 8$ while matching or exceeding baseline performance. Indeed, these experiments demonstrate that all the *hidden* layers in the GCN (i.e., dimensions d_1 and d_2 in this case) can be fully partitioned in GIST without observing a performance decrease, as long as we do not partition the input dimension; see Figure 2-(b).

How many Sub-GCNs to use? Increasing the number m of sub-GCNs used during GIST training typically improves training speed because *i*) sub-GCNs become smaller, *ii*) each sub-GCN is trained for fewer epochs, and *iii*) sub-GCNs are trained in parallel. As shown in Table 2, for practical values of m , the number of sub-GCNs does not seem to impact the performance of models trained with GIST on small-scale datasets. In fact, model performance often improves as the number of sub-GCNs is increased. Because increasing the number of sub-GCNs seems to maintain or improve model performance, one may continue increasing the number sub-GCNs, either until all available GPUs are occupied or model performance begins to decrease. The latter effect is more noticeable in large-scale experiments; see Tables 3 and A3.

Incorporating Local Iterations. GIST dictates that sub-GCNs be trained for a certain number ζ of independent, local iterations between synchronization rounds (Lin et al., 2018). Ideally, the number of local iterations should be maximized, thus decreasing the amount of communication for a fixed number of epochs. However, such reduced communication often comes at the cost of degraded model performance. We test GIST for different values of ζ ; see Figure 4. The performance of GIST is relatively robust to the number of local iterations, but test accuracy decreases slightly as ζ

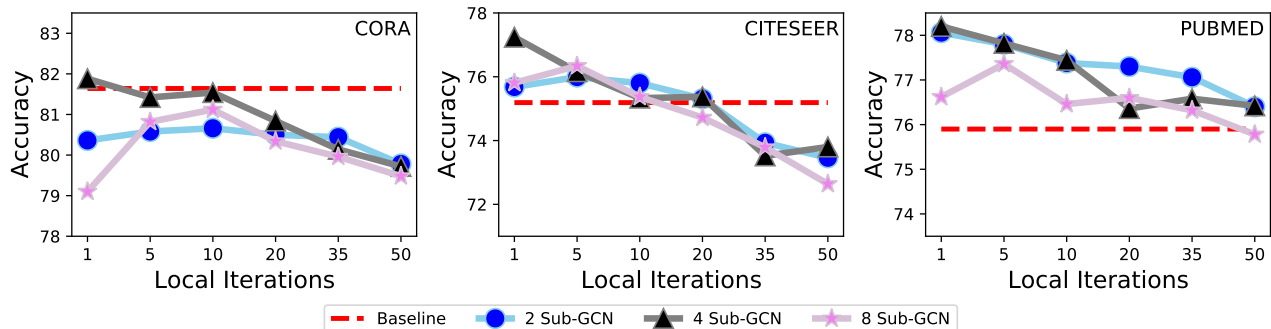


Figure 4. Performance of models trained with GIST on small-scale datasets for different numbers of local iterations and sub-GCNs in comparison to single-GPU baseline model performance.

increases. For small-scale datasets, using up to $\zeta = 20$ local iterations seems to perform consistently well for any number of sub-GCNs. However, for large-scale datasets, ζ can be further increased (e.g., $\zeta = 500$ or $\zeta = 5000$) without noticeable performance deterioration; see Section 4.2.

GIST Performance. Although GIST aims to achieve state-of-the-art performance (i.e., match the performance of single-GPU baseline models) while accelerating training, we have observed that GIST exceeds baseline performance in some cases. For example, in Figure 4, models trained with GIST outperform the baseline model for multiple experimental settings. Improved performance with GIST can be similarly observed in Table 2. Therefore, *the proposed methodology yields performance benefits in terms of both speed and accuracy*. Intuitively, we hypothesize that GIST yields improved accuracy because the process of randomly partitioning the global network into sub-GCNs throughout training, which loosely resembles dropout (Srivastava et al., 2014), provides regularization benefits. However, we leave an in-depth analysis of the performance benefits derived from GIST as future work.

4.2. Large-Scale Experiments

We perform experiments with GIST on Reddit (Hamilton et al., 2017) and Amazon2M datasets (Chiang et al., 2019), which are currently the largest, publicly-available datasets for machine learning on graphs.

Reddit Dataset. For the Reddit dataset, we adopt as baselines two, three, and four-layer GraphSAGE models (Hamilton et al., 2017) with hidden dimensions of 256. F1 score and training time are used to measure each model’s performance. All tests are run for a total of 80 epochs with no weight decay, using the Adam optimizer (Kingma & Ba, 2014). We find that $\zeta = 500$ achieves consistently high performance for GIST on Reddit. The training graph is partitioned into 15,000 sub-graphs during training and a batch size of 10 is used. Tests are repeated for three trials, and the average performance across trials is reported.

Table 3. Performance of GIST on the Reddit node classification dataset in comparison to single-GPU baseline models.

L	# Sub-GCNs	F1 Score	Time	Speedup
2	Baseline	96.09	105.78s	-
	2	96.40	70.29s	1.50 \times
	4	96.16	68.88s	1.54 \times
	8	95.46	76.68s	1.38 \times
3	Baseline	96.32	118.37s	-
	2	96.36	80.46s	1.47 \times
	4	95.76	78.74s	1.50 \times
	8	94.39	88.54s	1.34 \times
4	Baseline	96.32	120.74s	-
	2	96.01	91.75s	1.32 \times
	4	95.21	78.74s	1.53 \times
	8	92.75	88.71s	1.36 \times

The results of experiments on Reddit are provided in Table 3. GIST outperforms the single-GPU baseline model in terms of training time in all experimental settings. Moreover, for all model depths, the best F1 score among partitioned models ($m > 1$) is achieved when $m = 2$ sub-GCNs are considered. Using $m = 4$ sub-GCNs provides a further decrease in training time, but the F1 score also decreases slightly.

To better understand the relationship between training speed and the hyperparameters of GIST, in Figure 5 we plot the total training time as a function of local iterations ζ for different values of m . Any number of sub-GCNs can provide acceleration in comparison to the single-GPU baseline model if ζ is sufficiently large. As expected, as ζ increases, a greater training acceleration is observed, but this acceleration diminishes as the number of local iterations becomes too large. For the three studied settings, $\zeta = 500$ local iterations achieve nearly maximal training acceleration. Using four sub-GCNs slightly outperforms the two sub-GCN case with respect to total training time when $\zeta \geq 500$. Using eight sub-GCNs does not provide further acceleration. However, in cases where more computation is involved (e.g.,

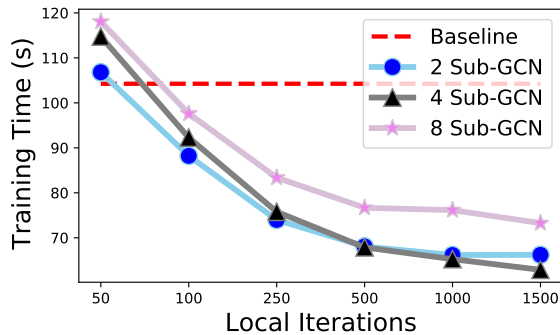


Figure 5. Total training time for GIST on Reddit as a function of the number of local iterations ζ and parameterized by the number of sub-GCNs m . The training time of a 2-layer single-GPU baseline model is provided for reference.

Table 4. Performance of GIST on the Amazon2M dataset with different hidden dimensions. Experiments marked with a “-” are excluded because training took more than 12 hours.

L	# Sub-GCNs	F1 Score (Time)	
		$d_i = 400$	$d_i = 4096$
2	Baseline	89.90 (6519.73s)	91.25 (18624.2s)
	2	88.36 (4485.33s)	90.70 (6109.88s)
	4	86.33 (4009.24s)	89.49 (4074.85s)
	8	84.73 (4061.81s)	88.86 (4003.87s)
	8	-	-
3	Baseline	90.36 (8367.09s)	91.51 (34278.6s)
	2	88.59 (5615.34s)	91.12 (7626.45s)
	4	86.46 (4917.64s)	89.21 (5103.69s)
	8	84.76 (4936.97s)	86.97 (4812.80s)
	8	-	-
4	Baseline	90.40 (10808.1s)	-
	2	88.56 (6443.53s)	91.02 (9966.33s)
	4	87.53 (5674.26s)	89.07 (5953.43s)
	8	85.32 (5601.51s)	87.53 (5596.43s)
	8	-	-

larger datasets or larger models), the use of eight sub-GCNs can further accelerate training, as can be seen in the experiments on the Amazon2M dataset.

Amazon2M Dataset. For the Amazon2M dataset, we follow the experimental settings of (Chiang et al., 2019). As our baseline, we adopt two, three, and four-layer GraphSAGE models (Hamilton et al., 2017) with hidden dimensions of 400 and 4096 (we refer to these models as “narrow” and “wide”, respectively). The training graph is partitioned into 15,000 sub-graphs and a batch size of 10 is used. Models are trained for 400 total epochs with the Adam optimizer (Kingma & Ba, 2014) and no weight decay. Performance is measured in terms of F1 score and training time. For all experiments with GIST, $\zeta = 5000$ local iterations are used, which we find to perform consistently well.

Results on the Amazon2M dataset are given in Table A3. All experiments reach the best accuracy in their last 16%

epochs, and many experiments reach top accuracy in the last 10% of epochs. For narrow models, GIST causes a slight performance decrease in comparison to the baseline, which is most noticeable when four or eight sub-GCNs are used. However, this degradation in performance is minor in many cases, and GIST provides a significant decrease in training speed. For example, when $L = 4$, GIST achieves a $\times 1.67$ speedup with 2 sub-GCNs, while decreasing F1 score by 2.

For wide models, GIST provides a more significant speedup. When $L = 2$, GIST completes training over $\times 3$ faster than the baseline. Furthermore, GIST with eight sub-GCNs achieves the largest speedup for all experiments with wide models, revealing that further acceleration can be achieved with GIST as the number of sub-GCNs is increased. Although the performance of GIST with eight sub-GCNs is worse than the baseline, the baseline takes significantly longer to achieve equal performance. For example, when $L = 2$, GIST with eight sub-GCNs achieves an F1 score of 88.86 in $\sim 4,000$ seconds, while the baseline takes roughly $\sim 10,000$ seconds to achieve a comparable F1 score.

GIST performance also improves with wider networks. For example, GIST with two sub-GCNs nearly matches baseline performance for wide GCNs, and eight sub-GCN GIST for wide networks outperforms two sub-GCN GIST for narrow networks. Generally, these trends in performance reveal that GIST performs best with wide GCN models.

Ultra-Wide GCNs. To illustrate the power of our proposed methodology, we leverage GIST to train a model of shocking scale on the Amazon2M dataset. Using identical experimental settings, we increase the width of the GCN model trained on Amazon2M to 32,768. It should be noted that this model is orders of magnitude wider than any GCN model ever explored in previous work. Due to the size of this model, evaluation of the full model cannot be performed even on the CPU with the entire graph. Therefore, the graph is partitioned during testing to avoid memory overflow, thus making the performance of this model worse and not comparable to the metrics provided in Table A3. For comparison, we find that the two-layer 4096-wide model trained using GIST with four sub-GCNs, which achieves an F1 score of 89.49 by standard evaluation shown in Table A3, gets 88.79 when evaluated using sub-graphs. Similarly, using GIST with four sub-GCNs, we train a 32K ultra-wide model to an F1 score of 89.73 in 17168 seconds. The ability to train a model of such scale over the largest-known dataset for node classification affirms the ability of GIST to enable large-scale experiments on graphs.

5. Conclusion

We presented GIST, a distributed approach that enables efficient training of wide GCNs on large graphs. GIST combines layer and graph sampling schemes to generate

several smaller sub-GCNs that are independently trained and intermittently aggregated into a global GCN model. We have shown that GIST achieves remarkable speed-ups in large graph datasets and even enables the training of GCN models of unprecedented size.

References

- Agarwal, A. and Duchi, J. C. Distributed delayed stochastic optimization. In *Proceedings of Advances in Neural Information Processing Systems (NeurIPS)*, 2011.
- Balaban, A. T. Applications of Graph Theory in Chemistry. *Journal of Chemical Information and Computer Sciences*, 1985.
- Ben-Nun, T. and Hoefler, T. Demystifying Parallel and Distributed Deep Learning: An In-Depth Concurrency Analysis. *ACM Computing Surveys (CSUR)*, 2019.
- Benkő, G., Flamm, C., and Stadler, P. F. A graph-based toy model of chemistry. *Journal of Chemical Information and Computer Sciences*, 2003.
- Bronstein, M. M., Bruna, J., LeCun, Y., Szlam, A., and Vandergheynst, P. Geometric Deep Learning: Going beyond Euclidean data. *IEEE Signal Processing Magazine*, 2017.
- Brown, T. B. et al. Language models are few-shot learners. *arXiv preprint arXiv:2005.14165*, 2020.
- Chen, J., Ma, T., and Xiao, C. FastGCN: Fast Learning with Graph Convolutional Networks via Importance Sampling. In *Proceedings of the International Conference on Learning Representations (ICLR)*, 2018a.
- Chen, J., Zhu, J., and Song, L. Stochastic Training of Graph Convolutional Networks with Variance Reduction. In *Proceedings of the International Conference on Machine Learning (ICML)*, 2018b.
- Chiang, W.-L., Liu, X., Si, S., Li, Y., Bengio, S., and Hsieh, C.-J. Cluster-gcn: An efficient algorithm for training deep and large graph convolutional networks. In *Proceedings of International Conference on Knowledge Discovery & Data Mining (KDD)*, 2019.
- Conneau, A., Khandelwal, K., Goyal, N., Chaudhary, V., Wenzek, G., Guzmán, F., Grave, E., Ott, M., Zettlemoyer, L., and Stoyanov, V. Unsupervised Cross-lingual Representation Learning at Scale. *arXiv preprint arXiv:1911.02116*, 2019.
- Defferrard, M., Bresson, X., and Vandergheynst, P. Convolutional neural networks on graphs with fast localized spectral filtering. *arXiv preprint arXiv:1606.09375*, 2016.
- Gao, H., Wang, Z., and Ji, S. Large-Scale Learnable Graph Convolutional Networks. *arXiv preprint arXiv:1808.03965*, 2018.
- Gholami, A., Azad, A., Jin, P., Keutzer, K., and Buluc, A. Integrated Model, Batch and Domain Parallelism in Training Neural Networks. *arXiv preprint arXiv:1712.04432*, 2017.
- Gori, M., Monfardini, G., and Scarselli, F. A new model for learning in graph domains. In *Proceedings of the IEEE International Joint Conference on Neural Networks (IJCNN)*, 2005.
- Günther, S., Ruthotto, L., Schroder, J. B., Cyr, E. C., and Gauger, N. R. Layer-Parallel Training of Deep Residual Neural Networks. *arXiv preprint arXiv:1812.04352*, 2018.
- Hamilton, W., Ying, Z., and Leskovec, J. Inductive representation learning on large graphs. In *Proceedings of Advances in Neural Information Processing Systems (NeurIPS)*, 2017.
- Huang, W., Zhang, T., Rong, Y., and Huang, J. Adaptive Sampling Towards Fast Graph Representation Learning. *arXiv preprint arXiv:1809.05343*, 2018.
- Karypis, G. and Kumar, V. A fast and high quality multilevel scheme for partitioning irregular graphs. *SIAM Journal on Scientific Computing*, 1998a.
- Karypis, G. and Kumar, V. Multilevelk-way partitioning scheme for irregular graphs. *Journal of Parallel and Distributed computing*, 1998b.
- Kingma, D. P. and Ba, J. Adam: A Method for Stochastic Optimization. *arXiv preprint arXiv:1412.6980*, 2014.
- Kipf, T. N. and Welling, M. Semi-Supervised Classification with Graph Convolutional Networks. *arXiv preprint arXiv:1609.02907*, 2016.
- Kirby, A. C., Samsi, S., Jones, M., Reuther, A., Kepner, J., and Gadepally, V. Layer-Parallel Training with GPU Concurrency of Deep Residual Neural Networks via Non-linear Multigrid. *arXiv preprint arXiv:2007.07336*, 2020.
- Lian, X., Zhang, C., Zhang, H., Hsieh, C.-J., Zhang, W., and Liu, J. Can Decentralized Algorithms Outperform Centralized Algorithms? A Case Study for Decentralized Parallel Stochastic Gradient Descent. In *Proceedings of Advances in Neural Information Processing Systems (NeurIPS)*, 2017.
- Lin, T., Stich, S. U., Kshitij Patel, K., and Jaggi, M. Don't Use Large Mini-Batches, Use Local SGD. *arXiv preprint arXiv:1808.07217*, 2018.

- Lusher, D., Koskinen, J., and Robins, G. *Exponential random graph models for social networks: Theory, methods, and applications*. Cambridge University Press, 2013.
- Masci, J., Boscaini, D., Bronstein, M., and Vandergheynst, P. Geodesic convolutional neural networks on riemannian manifolds. In *Proceedings of the IEEE International Conference on Computer Vision Workshops (ICCVW)*, 2015.
- Nakkiran, P., Kaplun, G., Bansal, Y., Yang, T., Barak, B., and Sutskever, I. Deep Double Descent: Where Bigger Models and More Data Hurt. *arXiv preprint arXiv:1912.02292*, 2019.
- Newman, M. E., Watts, D. J., and Strogatz, S. H. Random graph models of social networks. *Proceedings of the National Academy of Sciences*, 2002.
- Paszke, A. et al. Pytorch: An imperative style, high-performance deep learning library. In *Proceedings of Advances in Neural Information Processing Systems (NeurIPS)*, 2019.
- Pauloski, J. G., Zhang, Z., Huang, L., Xu, W., and Foster, I. T. Convolutional Neural Network Training with Distributed K-FAC. *arXiv preprint arXiv:2007.00784*, 2020.
- Sen, P., Namata, G., Bilgic, M., Getoor, L., Galligher, B., and Eliassi-Rad, T. Collective classification in network data. *AI magazine*, 29(3):93–93, 2008.
- Shi, S., Tang, Z., Chu, X., Liu, C., Wang, W., and Li, B. A Quantitative Survey of Communication Optimizations in Distributed Deep Learning. *arXiv preprint arXiv:2005.13247*, 2020.
- Srivastava, N., Hinton, G., Krizhevsky, A., Sutskever, I., and Salakhutdinov, R. Dropout: a simple way to prevent neural networks from overfitting. *Journal of Machine Learning Research (JMLR)*, 2014.
- Stich, S. U. Local SGD converges fast and communicates little. In *Proceedings of the International Conference on Learning Representations (ICLR)*, 2019.
- Tavarageri, S., Sridharan, S., and Kaul, B. Automatic Model Parallelism for Deep Neural Networks with Compiler and Hardware Support. *arXiv preprint arXiv:1906.08168*, 2019.
- Veličković, P., Cucurull, G., Casanova, A., Romero, A., Lio, P., and Bengio, Y. Graph attention networks. *arXiv preprint arXiv:1710.10903*, 2017.
- You, Y., Chen, T., Wang, Z., and Shen, Y. L2-gcn: Layer-wise and learned efficient training of graph convolutional networks. In *Proceedings of the IEEE Conference on Computer Vision and Pattern Recognition (CVPR)*, pp. 2127–2135, 2020.
- Yu, K., Flynn, T., Yoo, S., and D’Imperio, N. Layered sgd: A decentralized and synchronous sgd algorithm for scalable deep neural network training. *arXiv preprint arXiv:1906.05936*, 2019.
- Yuan, B., Kyrillidis, A., and Jermaine, C. M. Distributed Learning of Deep Neural Networks using Independent Subnet Training. *arXiv preprint arXiv:1810.01392*, 2019.
- Zeng, H., Zhou, H., Srivastava, A., Kannan, R., and Prasanna, V. GraphSAINT: Graph Sampling Based Inductive Learning Method. *arXiv preprint arXiv:1907.04931*, 2019.
- Zhang, S., Choromanska, A. E., and LeCun, Y. Deep learning with elastic averaging sgd. In *Proceedings of Advances in Neural Information Processing Systems (NeurIPS)*, 2015.
- Zhang, Z., Yin, L., Peng, Y., and Li, D. A quick survey on large scale distributed deep learning systems. In *2018 IEEE 24th International Conference on Parallel and Distributed Systems (ICPADS)*, 2018.
- Zhu, W., Zhao, C., Li, W., Roth, H., Xu, Z., and Xu, D. LAMP: Large Deep Nets with Automated Model Parallelism for Image Segmentation. *arXiv preprint arXiv:2006.12575*, 2020.
- Zinkevich, M., Weimer, M., Li, L., and Smola, A. J. Parallelized stochastic gradient descent. In *Proceedings of Advances in Neural Information Processing Systems (NeurIPS)*, pp. 2595–2603, 2010.
- Zou, D., Hu, Z., Wang, Y., Jiang, S., Sun, Y., and Gu, Q. Layer-Dependent Importance Sampling for Training Deep and Large Graph Convolutional Networks. *arXiv preprint arXiv:1911.07323*, 2019.

A. Comparison between Other Methods

A.1. Comparison to Local SGD

The major benefit of GIST arises from its communication-efficient methodology for disjointly partitioning the weights of a single, large GCN model across multiple machines for distributed training. A simple version of local SGD (Lin et al., 2018) could also be implemented for distributed training of GCNs by training the full model on each separate worker for a certain number of local iterations and intermittently averaging local updates. Similarly to GIST, this method would allow GCN training to be distributed across multiple GPUs, thus enabling some larger-scale experiments to be explored. However, GIST has superior communication-efficiency in comparison to local SGD, as only a fraction of model parameters are communicated to each machine. Furthermore, because each sub-GCN is smaller than the global model, GIST achieves an additional speedup during the local training of each sub-GCN in comparison to locally training the full model. To verify the efficiency benefits of GIST, we perform a direct comparison to local SGD over the Reddit dataset using a 2-layer GCN model with a hidden dimension of 256.

Table A1. Training metrics for two-layer GCN models with hidden dimension 256 trained using local SGD and GIST on the Reddit dataset. All models are trained with 100 local iterations for both GIST and local SGD.

# Machines	Method	F1 Score	Training Time
2	Local SGD	96.37	137.17s
	GIST	96.40	108.67s
4	Local SGD	95.00	127.63s
	GIST	96.16	116.56s
8	Local SGD	93.40	129.58s
	GIST	95.46	123.83s

GIST and local SGD are compared directly within Table A1. As can be seen, the combined effect of communicating fewer parameters and conducting training on smaller models allow GIST to accelerate training in comparison to local SGD. For example, in two machine setting, GIST completes training 20% faster than local SGD, even while achieving slightly improved test accuracy. In addition to providing a speedup in comparison to local SGD, GIST also provides higher test accuracy in all cases. Therefore, it is clear from these experiments that the GIST algorithm provides performance benefits on multiple fronts and is a viable alternative to local SGD for the distributed training of GCN models.

A.2. Comparison to Ensembles of Sub-GCNs

As previously mentioned, increasing the number of local iterations (i.e., ζ in Algorithm 1) decreases communication requirements given a fixed amount of training, thus yield-

Table A2. Training metrics for two-layer GCN models with hidden dimension of 256 on the Reddit dataset. Models are trained both with GIST and as ensembles of shallow sub-GCNs. The ensembles of shallow sub-GCNs are formed by partitioning the global model into sub-GCNs once, training them independently, and never aggregating their parameters into the global model.

# Machines	Method	F1 Score	Inference Time (s)
2	Ensemble	96.31	3.59
	GIST	96.40	1.81
4	Ensemble	96.10	6.38
	GIST	96.16	1.81
8	Ensemble	95.28	11.95
	GIST	95.46	1.81

ing an acceleration. When taken to the extreme (i.e., as $\zeta \rightarrow \infty$), one could minimize communication requirements by independently training sub-GCNs and never aggregating their parameters into the global model, thus forming an ensemble of sub-GCNs. To test whether such an ensemble is a viable alternative to GIST, the performance of such ensembles of sub-GCNs, in comparison to models trained with GIST, is presented in Table A2 for the Reddit dataset.¹ As can be seen, although training ensembles of sub-GCNs may minimize communication during training, such an approach yields inferior performance in comparison to GIST. Furthermore, because an entire ensemble of GCN models must be maintained, the inference time of the resulting model is significantly increased, which becomes more extreme as the number of sub-GCNs is increased (i.e., because more models exist within the ensemble).

B. More Details on Amazon2M Experiments

Comprehensive results on the Amazon2M dataset are given in Table A3. Compared to Table 4, explorations on more ultra-wide GCNs with GIST are conducted. Except for aggressively extending the width of the hidden layer to shocking values of 8K, 16K or even 32K, the experimental settings for ultra-wide GCN training are the same as the 400/4096 wide model. When d_i reaches 65,536, our machine suffers from out-of-memory error even using GIST with 8 sub-GCNs, which impedes our wider exploration.

Due to the size of ultra-wide models, we use GPU only for training. While testing, we use CPU to evaluate the full model on the entire graph. We mark the F1 score under the aforementioned method as “standard F1 score”. However, we find that when d_i goes beyond 4096, evaluation of the full model cannot be performed even on the CPU with the entire

¹For each sub-GCN, we measure validation accuracy throughout training and add the highest-performing model into the ensemble.

Table A3. Performance of GIST on the Amazon2M dataset with different hidden dimensions.

L	# Sub-GCNs	Standard / Sub-Graph F1 Score (Time)				
		$d_i = 400$	$d_i = 4096$	$d_i = 8192$	$d_i = 16384$	$d_i = 32768$
2	Baseline	89.90 / 89.38 (6519.73s)	91.25 / 90.58 (18624.2s)	-	-	-
	2	88.36 / 87.48 (4485.33s)	90.70 / 90.09 (6109.88s)	- / 90.87 (9940.67s)	- / 90.94 (33503.7s)	- / 90.91 (116315s)
	4	86.33 / 84.82 (4009.24s)	89.49 / 88.79 (4074.85s)	- / 89.76 (5373.88s)	- / 90.10 (8081.16s)	- / 90.17 (18567.7s)
	8	84.73 / 82.56 (4061.81s)	88.86 / 87.16 (4003.87s)	- / 88.31 (4322.39s)	- / 88.89 (5017.89s)	- / 89.46 (6339.79s)
3	Baseline	90.36 / 89.73 (8367.09s)	91.51 / 90.99 (34278.6s)	-	-	-
	2	88.59 / 87.79 (5615.34s)	91.12 / 90.40 (7626.45s)	- / 90.91 (17549.2s)	-	-
	4	86.46 / 85.30 (4917.64s)	89.21 / 88.51 (5103.69s)	- / 89.75 (7440.69s)	-	-
	8	84.76 / 82.84 (4936.97s)	86.97 / 86.12 (4812.80s)	- / 88.38 (4946.55s)	-	-
4	Baseline	90.40 / 89.77 (10808.1s)	91.61 / 91.02 (51110.0s)	-	-	-
	2	88.56 / 87.75 (6443.53s)	91.02 / 90.36 (9966.33s)	- / 91.08 (24901.5s)	-	-
	4	87.53 / 85.32 (5674.26s)	89.07 / 88.50 (5953.43s)	- / 89.76 (8493.98s)	-	-
	8	85.32 / 83.45 (5601.51s)	87.53 / 86.60 (5596.43s)	- / 88.13 (5787.04s)	-	-

graph. Therefore, the graph is partitioned into 5,000 sub-graphs during testing to avoid memory overflow, marked as “sub-graph F1 score”. Both standard F1 score and sub-graph F1 score are reported in Table A3.

From Table A3, we find that 2-layer-8196 model with 2 sub-GCNs GIST reaches higher accuracy than 2-layer-4096 baseline model, with the training duration cut half. It also achieves a comparable performance to 3-layer-4096 baseline model but with significantly $\times 4$ speed-up. Similarly, 4-layer-8192 model reaches the highest sub-graph F1 score across the table using 2 sub-GCNs GIST in 7 hours, whereas 4-layer-4096 model needs over 14 hours to get similar results.

Besides, we find that the model performance is generally proportional to the hidden dimensions, showing that the overparameterized GCN model, especially on width, has a positive effect on large-scale dataset Amazon2M. We also notice that the accuracy drop when applying GIST is relatively smaller when the hidden dimension is larger, which reflects that wider GCNs favor GIST.

C. Full Results on Reddit dataset

Here, we present all experimental settings that were tested on the Reddit dataset. These results are listed in Table A4. For each experiment, we include the optimal learning rate that was used to achieve the recorded results. Baseline experiments are excluded because all relevant baseline results are provided in the main text.

D. Full Results on Small Datasets

Here, we present several tables which contain the full results for all experimental settings that were tested on small-scale datasets (i.e., CORA, CITESEER, and PUBMED). These results are provided in Tables A5, A6, A7, and A8. For

each experiment, the optimal learning rate, which yielded top-performing results, is also listed. In the main text, the metric that is reported is the best test accuracy, but in these tables we also list the validation and final test accuracies for completeness.

Table A4. Performance of all experimental settings for 256-dimensional GraphSAGE (Hamilton et al., 2017) models trained with GIST on the Reddit dataset. All GIST experiments used weight decay of 0 and were trained for 80 epochs in total.

# Layers	ζ	# Sub-GCNs	LR	Best Test F1	Time (s)
2	100	2	0.01	96.43	109.57
		4	0.01	95.97	116.38
		8	0.01	94.41	123.14
	500	2	0.01	96.40	81.44
		4	0.005	96.16	78.75
		8	0.01	95.46	90.49
	1000	2	0.005	96.42	77.28
		4	0.01	96.20	73.86
		8	0.01	95.24	80.67
	1500	2	0.01	96.31	77.24
		4	0.01	96.10	71.34
		8	0.01	95.24	87.52
3	100	2	0.01	96.34	128.19
		4	0.01	95.33	140.45
		8	0.001	92.47	149.79
	500	2	0.005	96.36	95.41
		4	0.005	95.76	89.25
		8	0.01	94.39	97.82
	1000	2	0.005	96.39	91.01
		4	0.01	95.90	85.04
		8	0.01	95.01	90.59
	1500	2	0.005	96.18	86.46
		4	0.005	95.94	80.92
		8	0.01	95.01	91.67
4	100	2	0.005	96.13	145.27
		4	0.01	94.17	162.10
		8	0.01	84.07	177.06
	500	2	0.005	96.01	105.88
		4	0.005	95.21	99.92
		8	0.01	92.75	108.11
	1000	2	0.005	96.32	99.94
		4	0.005	95.73	96.63
		8	0.01	92.26	100.11
	1500	2	0.005	96.11	95.18
		4	0.01	95.80	92.39
		8	0.01	92.26	96.78

Table A5. Performance of single-GPU baseline models of different sizes on small-scale datasets.

Dataset	Depth	Width	LR	Best Test Acc.	Best Val Acc.	Last Test Acc.
CORA	2	16	0.05	79.00	77.40	75.40
	2	64	0.05	81.72	80.92	78.56
	2	128	0.05	82.30	80.96	79.36
	2	256	0.05	82.96	80.84	80.54
	2	512	0.05	81.54	79.88	79.44
	2	1024	0.01	81.18	80.32	79.94
	3	16	0.05	78.86	77.12	76.28
	3	64	0.05	81.08	79.24	76.70
	3	128	0.05	81.52	79.36	77.56
	3	256	0.01	81.64	79.48	78.60
	3	512	0.01	82.28	80.16	78.30
	3	1024	0.01	82.24	80.52	79.78
	4	16	0.1	78.70	77.68	75.92
	4	64	0.005	80.68	78.64	75.08
	4	128	0.01	80.76	79.64	76.98
	4	256	0.005	81.14	80.32	78.44
	4	512	0.005	81.88	79.80	77.62
	4	1024	0.005	79.86	78.16	76.62
CITeseer	2	16	0.05	72.53	71.46	67.50
	2	64	0.1	76.00	75.50	72.62
	2	128	0.05	76.68	76.24	72.87
	2	256	0.05	77.05	76.02	74.13
	2	512	0.05	76.10	75.78	74.14
	2	1024	0.05	76.10	75.88	73.94
	3	16	0.1	72.00	72.28	68.77
	3	64	0.05	75.08	74.30	70.75
	3	128	0.01	75.02	75.62	72.18
	3	256	0.005	75.19	75.32	73.16
	3	512	0.01	76.00	75.10	72.14
	3	1024	0.05	75.56	74.86	72.33
	4	16	0.1	71.55	70.86	69.10
	4	64	0.005	74.52	74.06	68.36
	4	128	0.01	74.26	73.88	70.67
	4	256	0.005	74.59	74.46	71.81
	4	512	0.005	74.66	73.42	71.09
	4	1024	0.005	72.39	71.96	69.50
PUBMED	2	16	0.05	74.22	73.65	69.79
	2	64	0.1	77.20	76.79	74.29
	2	128	0.1	77.45	77.23	75.09
	2	256	0.05	77.90	77.33	75.07
	2	512	0.1	77.33	76.99	75.52
	2	1024	0.05	77.18	77.12	75.11
	3	16	0.1	74.12	74.44	71.37
	3	64	0.1	76.01	75.68	72.63
	3	128	0.05	76.01	75.95	73.35
	3	256	0.05	75.90	76.07	73.63
	3	512	0.05	75.97	75.84	72.87
	3	1024	0.01	75.99	76.07	73.53
	4	16	0.1	74.12	74.44	71.37
	4	64	0.1	76.01	75.68	72.63
	4	128	0.005	75.34	75.57	72.59
	4	256	0.05	75.90	76.07	73.63
	4	512	0.05	75.97	75.84	72.87
	4	1024	0.01	75.99	76.07	73.53

Table A6. Performance of narrow three-layer GCN model (i.e., hidden dimension of 64) trained with GIST on small-scale datasets. These tests do not split the input layer, but they do split the output layer.

Dataset	ζ	# Sub-GCN	LR	Best Test Acc.	Best Val. Acc.	Last Test Acc.
CORA	1	2	0.1	80.24	78.92	76.64
	1	4	0.01	80.56	79.24	78.34
	1	8	0.01	76.34	74.60	69.98
	5	2	0.005	80.18	79.04	76.50
	5	4	0.01	79.34	77.56	77.86
	5	8	0.005	74.14	72.00	72.86
	10	2	0.05	80.06	79.00	77.80
	10	4	0.01	78.76	76.80	77.86
	10	8	0.005	73.22	72.20	73.18
	20	2	0.005	79.84	78.44	77.02
	20	4	0.005	79.24	77.68	78.84
	20	8	0.005	75.88	74.76	75.26
	30	2	0.05	79.44	78.88	78.14
	30	4	0.005	79.16	77.92	78.12
	30	8	0.05	76.16	74.40	60.72
CITSEER	1	2	0.05	76.28	76.10	70.87
	1	4	0.01	76.63	75.70	73.16
	1	8	0.01	74.82	73.44	70.23
	5	2	0.1	75.96	75.42	71.15
	5	4	0.005	75.55	74.98	73.72
	5	8	0.005	72.61	71.50	71.74
	10	2	0.1	76.11	74.96	73.43
	10	4	0.01	75.37	74.16	73.31
	10	8	0.005	71.94	71.08	71.92
	20	2	0.01	74.82	73.64	70.90
	20	4	0.1	74.99	74.20	74.10
	20	8	0.005	72.75	71.98	72.43
	30	2	0.1	74.62	74.06	73.01
	30	4	0.05	73.93	73.36	72.68
	30	8	0.005	71.76	70.80	71.65
PUBMED	1	2	0.1	77.02	77.20	69.97
	1	4	0.05	76.61	76.67	73.75
	1	8	0.01	74.32	73.93	70.37
	5	2	0.1	76.27	76.20	72.60
	5	4	0.01	75.99	75.76	74.90
	5	8	0.01	72.57	72.05	70.75
	10	2	0.1	76.31	75.71	73.80
	10	4	0.01	75.62	75.03	73.73
	10	8	0.005	70.97	70.80	70.79
	20	2	0.01	75.41	75.00	72.08
	20	4	0.1	75.40	74.83	74.43
	20	8	0.005	72.63	72.55	71.93
	30	2	0.1	75.26	74.88	73.72
	30	4	0.1	74.82	74.72	71.06
	30	8	0.01	72.02	71.60	69.62

Table A7. Performance of wide three-layer GCN model (i.e., hidden dimension 256) trained with GIST on small-scale datasets. These tests do not split the input layer, but they do split the output layer. Tests that do not split the output layer performed similarly.

Dataset	ζ	# Sub-GCN	LR	Best Test Acc.	Best Val. Acc.	Last Test Acc.
CORA	1	2	0.05	79.32	78.84	76.26
	1	4	0.01	79.80	78.68	76.28
	1	8	0.05	79.40	77.88	75.64
	5	2	0.1	79.80	78.44	75.54
	5	4	0.05	79.56	77.48	77.28
	5	8	0.05	78.20	76.60	77.56
	10	2	0.1	79.48	78.44	77.70
	10	4	0.01	78.80	77.80	76.88
	10	8	0.005	77.66	76.84	77.44
	20	2	0.1	79.24	78.08	77.16
	20	4	0.1	78.30	77.32	76.92
	20	8	0.01	77.22	75.24	76.94
	30	2	0.05	78.26	77.40	76.32
	30	4	0.01	78.18	76.76	78.08
	30	8	0.01	76.44	74.68	76.44
CITeseer	1	2	0.05	75.38	75.26	69.32
	1	4	0.1	75.89	75.12	68.35
	1	8	0.05	75.93	75.14	71.85
	5	2	0.1	75.63	74.42	69.60
	5	4	0.1	75.39	75.06	72.20
	5	8	0.05	75.06	74.42	72.91
	10	2	0.1	74.90	74.26	72.35
	10	4	0.1	74.93	74.62	73.22
	10	8	0.005	74.06	73.90	72.78
	20	2	0.1	74.18	73.54	71.47
	20	4	0.1	73.55	72.96	72.86
	20	8	0.005	73.51	73.20	72.66
	30	2	0.05	73.35	73.36	71.84
	30	4	0.1	72.95	72.82	72.71
	30	8	0.005	72.33	72.00	72.33
PUBMED	1	2	0.05	76.31	76.56	70.95
	1	4	0.05	76.51	76.55	71.55
	1	8	0.05	76.03	75.92	72.05
	5	2	0.1	76.38	75.69	71.15
	5	4	0.1	75.89	75.88	72.98
	5	8	0.05	74.91	74.97	72.98
	10	2	0.1	75.45	75.12	72.89
	10	4	0.1	75.45	75.45	73.93
	10	8	0.005	74.58	74.44	73.56
	20	2	0.1	74.89	74.61	72.72
	20	4	0.05	73.91	73.45	73.24
	20	8	0.05	73.99	73.81	73.21
	30	2	0.05	74.22	74.33	72.93
	30	4	0.1	73.87	74.05	73.33
	30	8	0.005	72.84	72.91	72.75

Table A8. Performance of wide three-layer GCN model (i.e., hidden dimension 256) on small-scale datasets trained with GIST. These tests split the input layer and the output layer.

Dataset	ζ	# Sub-GCN	LR	Best Test Acc.	Best Val. Acc.	Last Test Acc.
CORA	1	2	0.05	80.64	79.40	76.64
	1	4	0.05	79.60	78.36	76.28
	1	8	0.05	73.70	72.72	60.48
	10	2	0.1	79.18	79.24	76.86
	10	4	0.01	76.38	75.04	75.60
	10	8	0.01	62.08	60.36	61.56
	20	2	0.05	78.90	78.32	77.78
	20	4	0.01	76.56	74.80	76.56
	20	8	0.01	57.00	54.40	57.00
CITeseer	1	2	0.1	71.02	75.64	70.72
	1	4	0.05	75.82	74.68	72.43
	1	8	0.01	72.47	71.28	66.80
	10	2	0.1	74.96	75.26	72.60
	10	4	0.01	73.10	72.94	72.05
	10	8	0.01	63.77	63.00	63.16
	20	2	0.1	74.14	73.88	72.80
	20	4	0.01	72.67	71.36	71.63
	20	8	0.01	58.67	57.44	58.67
PUBMED	1	2	0.05	76.57	76.51	72.54
	1	4	0.1	75.52	75.67	71.55
	1	8	0.05	73.03	72.96	65.15
	10	2	0.1	75.52	75.73	73.53
	10	4	0.01	74.05	73.83	73.14
	10	8	0.01	65.51	65.55	64.81
	20	2	0.1	74.83	74.88	73.61
	20	4	0.01	73.45	73.08	72.51
	20	8	0.01	62.12	61.12	59.41
